

Learning Physics-Informed Neural Networks without Stacked Back-propagation

Di He^{1*}, Wenlei Shi^{1*}, Shanda Li^{2*}

Xiaotian Gao¹, Jia Zhang¹, Jiang Bian¹, Liwei Wang², Tie-Yan Liu¹

¹Microsoft Research ²Peking University

{dihe, wenshi, xiaotian.gao, zhangjia, jiang.bian, tyliu}@microsoft.com

{lishanda, wanglw}@pku.edu.cn

Abstract

Physics-Informed Neural Network (PINN) has become a commonly used machine learning approach to solve partial differential equations (PDE). But, facing high-dimensional second-order PDE problems, PINN will suffer from severe scalability issues since its loss includes second-order derivatives, the computational cost of which will grow along with the dimension during stacked back-propagation. In this paper, we develop a novel approach that can significantly accelerate the training of Physics-Informed Neural Networks. In particular, we parameterize the PDE solution by the Gaussian smoothed model and show that, derived from Stein’s Identity, the second-order derivatives can be efficiently calculated without back-propagation. We further discuss the model capacity and provide variance reduction methods to address key limitations in the derivative estimation. Experimental results show that our proposed method can achieve competitive error compared to standard PINN training but is two orders of magnitude faster.

1 Introduction

Partial Differential Equations (PDEs) play a prominent role in describing the governing physical laws underlying a given system. Finding the solution of PDEs is important in understanding and predicting the physical phenomena from the laws. Recently, researchers sought to solve PDEs via machine learning methods by leveraging the power of deep neural networks [21, 20, 29, 11, 31, 13]. One of the seminal works in this direction is the Physics-Informed Neural Networks (PINN) approach [29]. PINN parameterizes the solution as a neural network and learns the weights by minimizing some loss functional related to the PDEs, e.g., the PDE residual.

Although the framework is general to learn any PDEs, few previous works experimented with PINN on high-dimensional second-order PDE problems. By thorough investigation, we find PINN training suffers from a significant scalability issue, mainly resulting from stacked back-propagation. Note that the PDE residual loss contains second-order derivatives. To update the weights of the neural network by gradient descent, one must first perform automatic differentiation (i.e., back-propagation) multiple times to compute the derivatives in the PDE and then calculate the loss. For high-dimensional second-order PDEs, the computational cost in such stacked back-propagation grows along with increasing input dimension [27, 24]. This will result in considerable inefficiency, making the PINN approach impractical in large-scale settings. Since some fundamental PDEs in physics, such as the Schrodinger equations, are high-dimensional second-order PDEs, addressing the scalability issue of PINN becomes essential.

*Equal contribution.

In this paper, we take a first step to tackle the scalability issue of PINN by developing a novel approach to train the model without stacked back-propagation. Particularly, we parameterize the PDE solution $u(x; \theta)$ as a Gaussian smoothed model, $u(x; \theta) = \mathbb{E}_{\delta \sim \mathcal{N}(0, \sigma^2 \mathbf{I})} f(x + \delta; \theta)$, where u transforms arbitrary base network f by injecting Gaussian noise into input x . This transformation gives rise to a key property for u where its derivatives to the input can be efficiently calculated *without back-propagation*. Such property is derived from the well-known Stein’s Identity [32] that essentially tells that the derivatives of any Gaussian smoothed function u can be reformulated as some expectation terms of the output of its base f , which can be estimated using Monte Carlo methods.

To be concrete, given any PDE problem, we can replace the derivative terms in the PDE with Stein’s derivative estimators, calculate the (estimated) residual losses in the forward pass, and then update the weight of the parameters via one-time back-propagation. Our method can accelerate the training of PINN from two folds of advantages. First, after using Stein’s derivative estimators, we no longer need stacked back-propagation to compute the loss, therefore saving significant computation time. Second, since the new loss calculation only requires forward-pass computation, it is quite natural to parallelize the computation into distributed machines to further accelerate the training.

Another point worth noting for the practical application of this method lies in the model capacity, which is highly related to the choice of the Gaussian noise level σ . We show that for large σ , the induced Gaussian smoothed models may not be expressive enough to approximate functions (i.e., learn solutions) with a large Lipschitz constant. Therefore, using a small value of σ is usually a better choice in practice. However, a small σ will lead to high-variance Stein’s derivative estimation, which inevitably causes unstable training. We introduce several variance reduction methods that have been empirically verified to be effective for mitigating the problem. Further experiments demonstrate that, compared to standard PINN training, our proposed method can achieve competitive error but is two orders of magnitude faster.

2 Related Work

2.1 Neural Approximation of PDE Solutions

Neural approximation approaches rely on governing equations and boundary conditions (or variants) to train neural networks to approximate the corresponding PDE solutions. Physics-Informed Neural Networks (PINN) [31, 29] is one of the typical learning frameworks which constrains the output of deep neural networks to satisfy the given governing equations and boundary conditions. The application of PINN includes aerodynamic flows [23, 35], power systems [25], and nano optic [3]. Recently, there is also a growing body of works on studying the optimization and generalization properties of PINN. [30] proved that the learned PINN will converge to the solution under certain conditions. [15] proposed to use curriculum regularization to avoid failures during PINN training. Different from the neural operator approaches [22, 18], the neural approximation methods can work in an unsupervised manner, without the need of labeled data generated by conventional PDE solvers.

2.2 Better Training for Physics-Informed Neural Networks

Despite the success of using PINN in solving various PDEs, researchers recently observed its training inefficiency in multiple aspects. For example, [12] discussed the architecture-wise inefficiency and introduced an adaptive activation function, which optimizes the network by dynamically changing the topology of the PINN loss function for different PDEs. The most relevant works related to our approach are [31] and [4], both of which tried to tackle the inefficiency in automatic differentiation by using numerical differentiation. In [31], a Monte Carlo approximation method is proposed to estimate the numerical differentiation of second-order derivatives for some specific second-order PDEs. Concurrently to our work, [4] introduced a method, which combines both auto-differentiation and numerical differentiation in PINN training to trade-off numerical truncation error and training efficiency. Compared to these two works, our designed approach can be applied to general PDEs and provide unbiased estimations of any derivatives without the need of back-propagation in the computation of the loss. Detailed discussions can be found in Section 4.3.

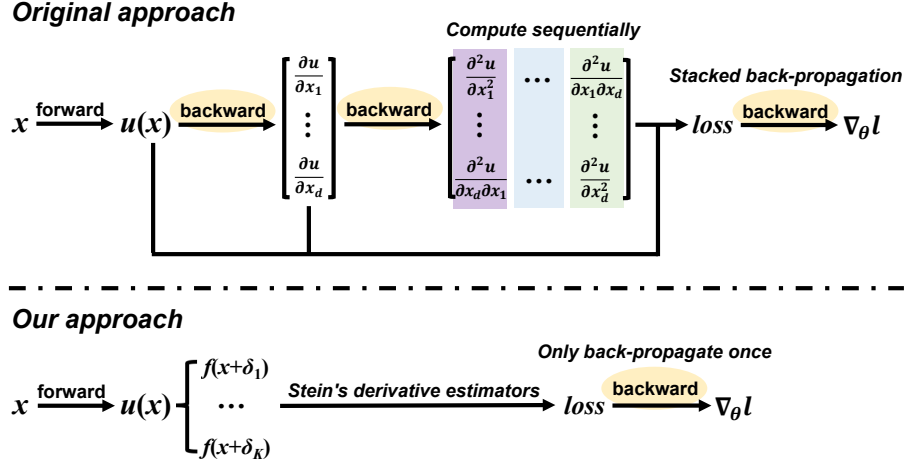


Figure 1: **Training process of the original PINN approach and our approach.** The original approach requires multiple backward passes to compute the derivative terms in the loss. By contrast, our approach leverages the *Stein's derivative estimators* to compute the loss without back-propagation.

2.3 Gaussian Smoothed Model

Injecting Gaussian noise to the input has been popularly used in machine learning to improve model generalization and robustness. Some works used Gaussian noise as a kind of data augmentation to improve the generalization ability of the learned model [1, 16], including denoising auto-encoder in image generation [33] and SimCLR in image pre-training [2]. Some works used Gaussian smoothed models for the sake of robustness guarantee. [17, 5] first used Gaussian smoothed models (a.k.a. randomized smoothing) to provide robustness guarantee when facing adversarial attacks. Since then, the smoothed models with different noise types have been developed for various scenarios [36, 34]. Leveraging Stein's Identity for efficient derivative estimation is not entirely new in machine learning. The method is one of the standard approaches in zero-order optimization where the exact derivatives cannot be obtained [8, 26, 19, 27]. To the best of our knowledge, there is no previous work using Stein's Identity on Gaussian smoothed models for efficient PINN training.

3 Preliminary

Without loss of generality, we formulate any partial differential equation as:

$$\mathcal{L}u(x) = \phi(x), \quad x \in \Omega \subset \mathbb{R}^d \quad (1)$$

$$\mathcal{B}u(x) = 0, \quad x \in \partial\Omega, \quad (2)$$

where \mathcal{L} is the partial differential operator and \mathcal{B} is the boundary condition. We use x to denote the spatiotemporal-dependent variable, and use u as the solution of the problem.

3.1 PINN Basics

Physics-informed Neural Networks (PINN) [29] is a popular choice to learn the function $u(x)$ automatically by minimizing the loss function induced by the governing equation (1) and boundary condition (2). To be concrete, given neural network $u(x; \theta)$ with parameter $\theta \in \Theta$, we define

$$l_{\Omega}[\theta] = \|\mathcal{L}u(x; \theta) - \phi(x)\|_{L^2(\Omega)} \quad (3)$$

$$l_{\partial\Omega}[\theta] = \|\mathcal{B}u(x; \theta)\|_{L^2(\partial\Omega)}. \quad (4)$$

The loss term $l_{\Omega}[\theta]$ in Eqn. (3) corresponds to the PDE residual, which evaluates how $u(x; \theta)$ fits the partial differential equation, and $l_{\partial\Omega}[\theta]$ in Eqn. (4) corresponds to the boundary residual, which measures how well $u(x; \theta)$ satisfies the boundary condition. It is easy to see, if there exists θ^* that

achieves zero loss in both residual terms $l_\Omega[\theta]$ and $l_{\partial\Omega}[\theta]$, then $u(x; \theta^*)$ will be a solution to the problem.

To find θ^* efficiently, PINN approaches leverage gradient-based optimization methods towards minimizing a linear combination of the two losses defined above. As the domain Ω and its boundary $\partial\Omega$ are usually continuous, Monte Carlo methods are used to approximate $l_\Omega[u]$ and $l_{\partial\Omega}[u]$ in practice. As a consequence, the optimization problem will be defined as

$$\arg \min_{\theta \in \Theta} \hat{l}_\Omega[\theta] + \lambda \hat{l}_{\partial\Omega}[\theta]. \quad (5)$$

In Eqn. (5),

$$\begin{aligned} \hat{l}_\Omega[\theta] &= \frac{1}{N_1} \sum_{i=1}^{N_1} \|\mathcal{L}u(x^{(i)}) - \phi(x^{(i)})\|_2, \\ \hat{l}_{\partial\Omega}[\theta] &= \frac{1}{N_2} \sum_{i=1}^{N_2} \|\mathcal{B}u(\tilde{x}^{(i)})\|_2, \end{aligned}$$

where $\{x^{(1)}, \dots, x^{(N_1)}\}$ and $\{\tilde{x}^{(1)}, \dots, \tilde{x}^{(N_2)}\}$ are i.i.d sampled over Ω and $\partial\Omega$, N_1 and N_2 are the respective sample sizes, and λ is the coefficient used to balance the interplay between the two loss terms.

3.2 Inefficiency of PINN

It can be seen that the loss for PINN training, as shown in Eqn. (5), is defined on the network's derivatives. Therefore, the computation of this loss requires multiple back-propagation steps, which can be very inefficient, especially for high-dimensional high-order PDE problems. In details, there are two sources of inefficiency in computing the PINN loss. The first one lies in the order-level inefficiency due to the fact that different orders of derivatives can only be calculated sequentially: One has to first build up the computational graph for the first-order derivatives and then perform back-propagation on this graph to obtain the second-order derivatives.

The second source is the dimension-level inefficiency which is a major issue for high-order PDE problems. In modern deep learning frameworks like PyTorch [28], one has to perform back-propagation on the computational graph sequentially for each partial derivative to implement second-order operators like the Laplace operator, leading to a computational cost proportional to the dimensionality of the input [27, 24].

Both of these two sources of inefficiency lead to a non-parallelizable training process, making the learning of PINN for high-dimensional high-order problems particularly slow. This issue will be much more serious for solving high-order PDE problems. Therefore, it becomes substantially beneficial to explore new parallelizable methods for PINN training since it may largely increase the training efficiency by making full use of advanced computing hardware, such as GPU.

4 Method

In this work, we propose a novel method which enables fully parallelizable PINN training. The key of our approach is using a specific formulation of $u(x; \theta)$:

$$u(x; \theta) = \mathbb{E}_{\delta \sim \mathcal{N}(0, \sigma^2 \mathbf{I})} f(x + \delta; \theta), \quad (6)$$

where $f(\cdot; \theta)$ is a neural network with parameter θ , and σ is the noise level of the Gaussian distribution. When queried at x , u returns the expected output of f when its input is sampled from a Gaussian distribution $\mathcal{N}(x, \sigma^2 \mathbf{I})$ centered at x . It can be easily seen that $u(x; \theta)$ is a ‘‘smoothed’’ network constructed from a ‘‘base’’ network $f(x; \theta)$ by injecting Gaussian noise into the input, and we call $u(x; \theta)$ a *Gaussian smoothed model*. For simplicity, we may omit θ and refer to the base network and the Gaussian smoothed model as $f(x)$ and $u(x)$ in the rest part of the paper.

4.1 Back-propagation-free Derivative Estimators

At first glance, using formulation (6) brings more difficulties since the output of u can only be estimated by repeatedly sampling δ . However, we show that the efficiency can be significantly

improved during training since all derivatives, as derived by Stein’s Identity, can be calculated in parallel without using back-propagation.

Theorem 1 (Stein’s Identity [32]). *Suppose $x \in \mathbb{R}^d$. For any measurable function $f(x)$, define $u(x) = \mathbb{E}_{\delta \sim \mathcal{N}(0, \sigma^2 \mathbf{I})} f(x + \delta)$, then we have $\nabla_x u = \mathbb{E}_{\delta \sim \mathcal{N}(0, \sigma^2 \mathbf{I})} [\frac{\delta}{\sigma^2} f(x + \delta)]$.*

For completeness, we give a short proof here.

Proof. Note that $u(x) = (2\pi)^{-\frac{n}{2}} \int_{\mathbb{R}^d} e^{-\frac{\|\delta\|^2}{2\sigma^2}} f(x + \delta) d\delta = (2\pi)^{-\frac{n}{2}} \int_{\mathbb{R}^d} e^{-\frac{\|t-x\|^2}{2\sigma^2}} f(t) dt$. We have $\nabla_x u(x) = (2\pi)^{-\frac{n}{2}} \int_{\mathbb{R}^d} \nabla_x e^{-\frac{\|t-x\|^2}{2\sigma^2}} f(t) dt = (2\pi)^{-\frac{n}{2}} \int_{\mathbb{R}^d} \frac{t-x}{\sigma^2} e^{-\frac{\|t-x\|^2}{2\sigma^2}} f(t) dt = \mathbb{E}_{\delta \sim \mathcal{N}(0, \sigma^2 \mathbf{I})} [\frac{\delta}{\sigma^2} f(x + \delta)]$, which completes the proof. \square

From the above theorem, we can see that the first-order derivative $\nabla_x u$ can be reformulated as an expectation term $\mathbb{E}_{\delta \sim \mathcal{N}(0, \sigma^2 \mathbf{I})} [\frac{\delta}{\sigma^2} f(x + \delta)]$. To calculate the value of the expectation, we can use Monte Carlo method to obtain an unbiased estimation from K i.i.d Gaussian samples, i.e.,

$$\nabla_x u \approx \frac{1}{K} \sum_{k=1}^K \frac{\delta_k}{\sigma^2} f(x + \delta_k), \delta_k \sim \mathcal{N}(0, \sigma^2 \mathbf{I}), k = 1, \dots, K. \quad (7)$$

It is easy to check that Stein’s Identity can be extended to any order of derivatives by recursion. Here we showcase the corresponding identity for Hessian matrix and Laplace operator:

- Hessian matrix $\mathbf{H}u$.

$$\mathbf{H}u = \mathbb{E}_{\delta \sim \mathcal{N}(0, \sigma^2 \mathbf{I})} \left[\left(\frac{\delta \delta^\top - \sigma^2 \mathbf{I}}{\sigma^4} \right) f(x + \delta) \right].$$

- Laplace operator Δu .

$$\Delta u = \mathbb{E}_{\delta \sim \mathcal{N}(0, \sigma^2 \mathbf{I})} \left[\left(\frac{\|\delta\|^2 - \sigma^2 d}{\sigma^4} \right) f(x + \delta) \right].$$

For convenience, we refer to the Monte Carlo estimators based on these identities as *vanilla Stein’s derivative estimators*.

We can plug the Stein’s derivative estimators into the physics-informed loss functions (Eqn. 5) defined for a given PDE. In this way, we are able to overcome the two sources of inefficiency in training PINN mentioned earlier. First, we can see that Stein’s derivative estimators for higher-order derivatives no longer require pre-computation for lower-order ones. This enables us to compute derivative terms of different orders in parallel instead of calculating them sequentially. Second, our method can address the dimension-level inefficiency for high-dimensional PDE problems. Using Stein’s derivative estimators, the derivatives with respect to each dimension can be obtained in a forward pass simultaneously instead of computing them dimension by dimension. See Figure 1 for an illustration of our approach.

These properties of Stein’s derivative estimators are appealing because they enable a fully-parallelizable PINN training and lead to significant improvement over efficiency for solving high-dimensional PDEs. In the meantime, a natural concern about the deficient expressiveness of Gaussian smooth function may rise. In the following subsection, we will take deep discussion on this issue and demonstrate the importance of σ in practice to control the model expressiveness.

4.2 Model Capacity

In our method, Gaussian smoothed neural network is used instead of vanilla neural network as the solution of PDE. This modification brings a natural concern, i.e., whether the function space of the proposed Gaussian smoothed models is expressive enough to approximate the solutions of a given PDE problem. In this subsection, we show that the capacity of Gaussian smoothed neural networks is closely related to the Lipschitz function class according to the following theoretical result:

Theorem 2. *For any measurable function $f : \mathbb{R}^d \rightarrow \mathbb{R}$, define $u(x) = \mathbb{E}_{\delta \sim \mathcal{N}(0, \sigma^2 \mathbf{I})} f(x + \delta)$, then $u(x)$ is $\frac{F}{\sigma} \sqrt{\frac{2}{\pi}}$ -Lipschitz with respect to ℓ_2 -norm, where $F = \sup_{x \in \mathbb{R}^d} |f(x)|$.*

Proof. Theorem 1 states that $\nabla_x u = \mathbb{E}_{\frac{\delta}{\sigma^2}} f(x + \delta)$.

Thus, for any unit vector α , we have

$$|\alpha^\top \nabla_x u| \leq \frac{1}{\sigma^2} \mathbb{E} |\alpha^\top \delta f(x + \delta)| \leq \frac{F}{\sigma^2} \mathbb{E} |\alpha^\top \delta| = \frac{F}{\sigma} \sqrt{\frac{2}{\pi}}.$$

The last equality holds since $\alpha^\top \delta \sim \mathcal{N}(0, \sigma^2)$. \square

Theorem 2 indicates that the noise level σ is an important hyper-parameter that controls the expressive power of the model $u(x)$. For example, if the neural network f uses sigmoid activation in the final prediction layer, its output range will be restricted to $(0, 1)$. From Theorem 2, it is straightforward to see that the Lipschitz constant of u is no more than $\frac{1}{\sigma} \sqrt{\frac{2}{\pi}}$ no matter how complex the network f is. In this setting, if we have a prior that the solution of a PDE has a large Lipschitz constant, we have to choose a small value of σ to approximate it well.

On the other hand, using small σ would affect the finite-sample approximation error of vanilla Stein’s derivative estimators. Without further assumptions on f , it is easy to check that the variance of vanilla Stein’s derivative estimators in Eqn. (7) can be inversely proportional to σ . Thus, naively using Monte Carlo method requires a large sample size for small σ , which may even slow down the training in practice. In the next subsection, we present several variance reduction approaches that we find particularly useful during training.

4.3 Variance-Reduced Stein’s Derivative Estimators

We mainly use two methods to reduce the variance for Stein’s derivative estimators, the control variate method and the antithetic variable method. For simplicity, we demonstrate how to apply the two techniques to improve the estimator of $\nabla_x u$ and Δu , which can be easily extended to other Stein’s derivative estimators.

The control variate method. One generic approach to reducing the variance of Monte Carlo estimates of integrals is to use an additive control variate [6, 7, 10], which is known as *baseline*. In our problem, we find $f(x)$ is a proper baseline which can lead to low-variance estimates of the derivative:

$$\nabla_x u = \mathbb{E}_{\delta \sim \mathcal{N}(0, \sigma^2 \mathbf{I})} \left[\frac{\delta}{\sigma^2} (f(x + \delta) - f(x)) \right] \approx \frac{1}{K} \sum_{k=1}^K \left[\frac{\delta_k}{\sigma^2} (f(x + \delta_k) - f(x)) \right]; \quad (8)$$

$$\Delta u = \mathbb{E} \left[\left(\frac{\|\delta\|^2 - \sigma^2 d}{\sigma^4} \right) (f(x + \delta) - f(x)) \right] \approx \frac{1}{K} \sum_{k=1}^K \left[\left(\frac{\|\delta_k\|^2 - \sigma^2 d}{\sigma^4} \right) (f(x + \delta_k) - f(x)) \right], \quad (9)$$

where δ_k are i.i.d. samples from $\mathcal{N}(0, \sigma^2 \mathbf{I})$. To see clearly why this technique leads to variance reduction, we take Eqn. (8) as an example. we assume $f(x)$ is smooth leverage its Taylor expansion at x to rewrite $\frac{\delta}{\sigma^2} (f(x + \delta) - f(x))$ as $\frac{\delta}{\sigma^2} (\delta^\top \nabla f(x) + o(\|\delta\|))$. This expression can be further simplified to $\xi^\top \nabla f(x) + o(1)$, where $\xi = \delta/\sigma \sim \mathcal{N}(0, \mathbf{I})$. Therefore, the variance of the estimator in Eqn. (8) will be *independent* of σ . This fact is in sharp contrast to the original estimator provided in Eqn. (7). With a similar argument, we can also show that the variance of the estimator in Eqn. (9) is inversely of proportional to σ , while the the variance of the original estimator for Δu is inversely proportional to σ^2 .

Further improvement using the antithetic variable method. The antithetic variable method is yet another powerful technique for variance reduction [9]. By using the symmetry of Gaussian distribution, it’s easy to see that Eqn. (8) and (9) still holds when δ is substituted with $-\delta$, which leads to new estimators. Averaging the new estimator and the one in Eqn. (8) / (9) gives the following

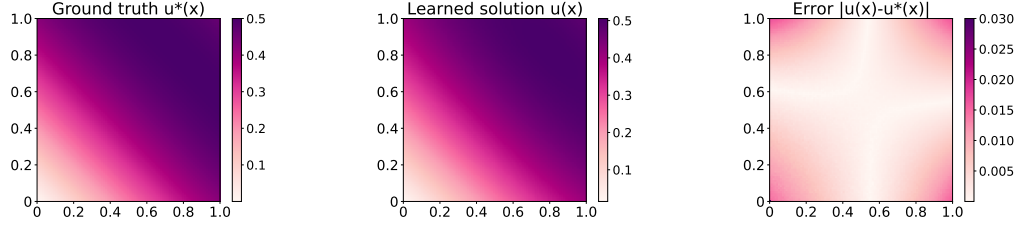


Figure 2: **Visualization for two-dimensional Poisson's Equation.** Three subfigures show the ground truth $u^*(x)$, the learned solution $u(x)$ and the point-wise error $|u(x) - u^*(x)|$ respectively.

result:

$$\nabla_x u = \mathbb{E} \left[\frac{\delta}{2\sigma^2} (f(x + \delta) - f(x - \delta)) \right] \approx \frac{1}{K} \sum_{k=1}^K \left[\frac{\delta_k}{2\sigma^2} (f(x + \delta_k) - f(x - \delta_k)) \right]; \quad (10)$$

$$\begin{aligned} \Delta u &= \mathbb{E} \left[\left(\frac{\|\delta\|^2 - \sigma^2 d}{2\sigma^4} \right) (f(x + \delta) + f(x - \delta) - 2f(x)) \right] \\ &\approx \frac{1}{K} \sum_{k=1}^K \left[\left(\frac{\|\delta_k\|^2 - \sigma^2 d}{2\sigma^4} \right) (f(x + \delta_k) + f(x - \delta_k) - 2f(x)) \right], \end{aligned} \quad (11)$$

Again, by leveraging the Taylor expansion of $f(x)$, one can show that the variances of the estimators in Eqn. (10) and (11) are both *independent* of σ . For example, $\left(\frac{\|\delta\|^2 - \sigma^2 d}{2\sigma^4} \right) (f(x + \delta) + f(x - \delta) - 2f(x)) = \left(\frac{\|\delta\|^2 - \sigma^2 d}{2\sigma^4} \right) (\delta^\top \mathbf{H} f(x) \delta + o(\|\delta\|^2))$, where $\mathbf{H} f(x)$ denotes the Hessian matrix of f at x . By letting $\xi = \delta/\sigma \sim \mathcal{N}(0, \mathbf{I})$, the estimator is simplified to $(\|\xi\|^2 - d)(\xi^\top \mathbf{H} f(x) \xi + o(1))$. Thus, its variance is *independent* of σ . This property is especially appealing because it enables us to tune model expressiveness according to PDE complexity in practice. For instance, we can use a small σ to ensure the model is expressive enough to learn a complex PDE solution.

We also provide empirical comparisons between vanilla Stein's derivative estimators and the improved ones. See Section 5.3 for details.

Note that Eqn. (8) and (11) look very similar to numerical differentiation in the surface form but they yield substantial differences. First, the roles of the term $f(x)$ are different. In Eqn. (8) and (11), the term $f(x)$ is introduced as the baseline which doesn't change the value of the expectation since $\mathbb{E} \left[\frac{\delta}{\sigma^2} f(x) \right] = \mathbb{E} \left[\left(\frac{\|\delta\|^2 - \sigma^2 d}{\sigma^4} \right) f(x) \right] = 0$. Therefore, multiplying any constant to $f(x)$ also holds, which will be infeasible for numerical differentiation. Second, our method provides unbiased estimation of the derivatives while numerical method can only obtain biased derivatives due to truncation error. Lastly, for d -dimensional derivative, numerical differentiation usually needs d samples (e.g., coordinate vectors) to obtain the derivative, while empirically we observe our method only requires a sample size much smaller than d in the following experiment section.

5 Experiments & Results

We conduct experiments to verify the effectiveness of our approach on a variety of PDE problems. Ablation studies on the design choices and hyper-parameters are then provided. Our codes are implemented based on PyTorch [28]. All the models are trained on one NVIDIA Tesla P100 GPU with 16GB memory and the reported training time is also measured on this machine.

5.1 Low-dimensional Problems

We first showcase our approach on two-dimensional PDE problems with visualization. In particular, we study the following two-dimensional Poisson's Equation with Dirichlet boundary conditions:

$$\begin{cases} \Delta u(x) = g(x) & x \in \Omega \\ u(x) = h(x) & x \in \partial\Omega \end{cases}$$

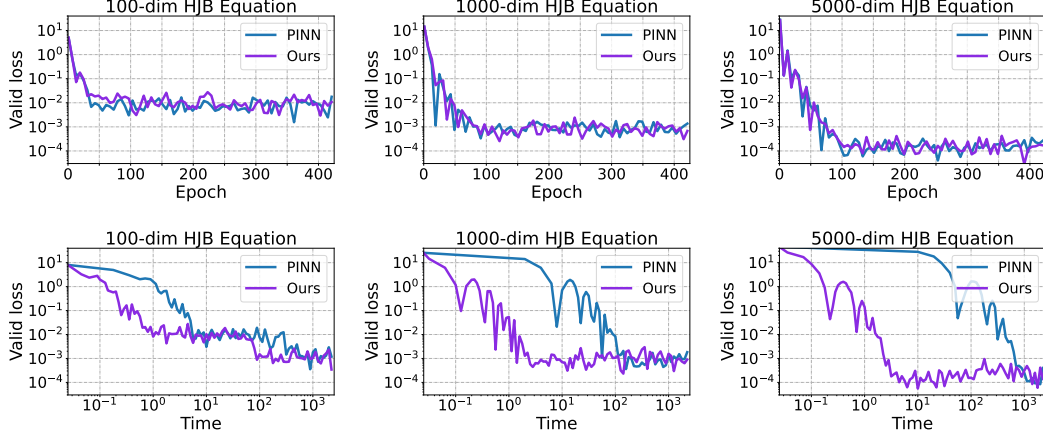


Figure 3: **Loss curves for high-dimensional HJB Equations.** In the top three subfigures, the x -axis indicates the epoch number. In the bottom three subfigures, the x -axis indicates the logarithmic-scaled training time. In all the subfigures, the y -axis indicates the logarithmic-scaled validation loss.

In our experiment, we set $\Omega = [0, 1]^2$, $g(x) = -\sin(x_1 + x_2)$ and $h(x) = \frac{1}{2} \sin(x_1 + x_2)$. This PDE has a unique solution $u^*(x) = \frac{1}{2} \sin(x_1 + x_2)$.

We train a Gaussian-smoothed model to fit the solution with our method. Specifically, the base neural network of our model is a 5-layer MLP with 100 neurons and tanh activation in each hidden layer. In our Gaussian smoothed model, the noise level σ is set to 0.1, and the number of samples K is set to 1024. We use the variance-reduced derivative estimator in Eqn. (11) based on the control variate method and the antithetic variable method. To train the model, we use Adam as the optimizer [14]. The learning rate is set to $1e-3$ in the beginning and then decays linearly to zero during training. In each training iteration, we sample $N_1 = 100$ points from the domain Ω and $N_2 = 100$ points from the boundary $\partial\Omega$ to obtain a mini-batch. Evaluations are performed on a hold-out validation set which is unseen during training. Evaluation metrics include the loss on the validation set and the mean squared error (MSE) with respect to the ground truth $u^*(x)$.

After training, our model reaches a validation loss of $1e-3$ and an MSE of $5e-5$, indicating that the model fits the ground truth well. We also examine the quality of the learned solution $\hat{u}(x)$ by visualization. Figure 2 shows the ground truth $u^*(x)$, the learned solution $u(x)$ and the point-wise error $|u(x) - u^*(x)|$. We can see that the point-wise error is less than $5e-3$ for most areas, thus the model can approximate the solution to Poisson’s Equation with high accuracy when using our method.

5.2 High-dimensional Hamilton-Jacobi-Bellman Equation

We use the high-dimensional Hamilton-Jacobi-Bellman (HJB) Equation to showcase the efficiency of our proposed method. HJB equation is an important non-linear PDE in optimal control theory. Its discrete-time counterpart is the Bellman equation widely used in reinforcement learning.

Experimental Design. Following [11], we study the classical linear-quadratic Gaussian (LQG) control problem in N dimensions, whose HJB equation is a second-order PDE² defined as below:

$$\begin{cases} u_t + \Delta u - \lambda \|\nabla_x u\|^2 = 0 & x \in [0, L]^N, t \in [0, T] \\ u(T, x) = g(x) & x \in [0, L]^N \end{cases}$$

We set the terminal condition $g(x) = \ln((1 + \|x\|^2)/2)$, the maximum value of the time $T = 1.0$, the maximum value of the state $L = 1.0$ and the parameter $\lambda = 1.0$.

²In Eqn. (1), x is defined as the spatiotemporal-dependent variable in the PDE for better presentation. Here in the HJB equation, we separately use x as the spatial-dependent variable and use t as the temporal-dependent variable. We hope this abuse of notations will not confuse the readers.

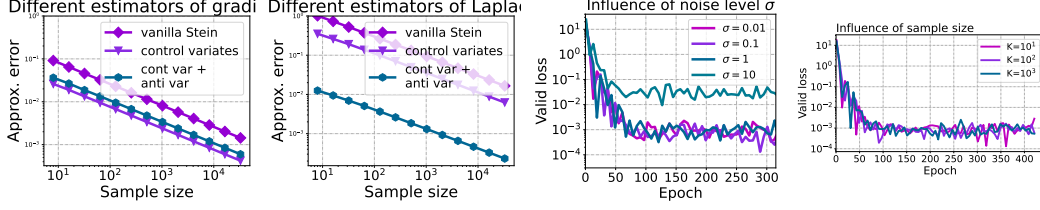


Figure 4: **Experimental results in ablation studies.** The first two subfigures show the approximation error of different estimators for the gradient and the Laplace operator, where the x -axis indicates the logarithmic-scaled sample sizes and the y -axis indicates the logarithmic-scaled approximation error. The last two subfigures show the loss curves of 1000-dimensional HJB Equation with varying noise levels and sample sizes, where the x -axis indicates the epoch number and the y -axis indicates the logarithmic-scaled validation loss.

To evaluate the training speed and performance in high dimensional cases, we compare our method with the original PINN approach given $N = 100, 1000$, and 5000 . In each training iteration, we sample $N_1 = 100$ points from the domain $[0, T] \times [0, L]^N$ and $N_2 = 100$ points from the boundary $[0, L]^N$ to obtain a mini-batch. The architecture of the Gaussian smoothed model and other training configurations are the same as those in Section 5.1. We use the variance-reduced derivative estimator in Eqn. (10) and (11) based on the control variate method and the antithetic variable method in all experiments. Evaluations are performed on a hold-out validation set which is unseen during training.

Experimental Results. Figure 3 shows the validation loss curves of both our method and the original PINN approach. In the figure, the x -axis indicates the epoch/time and the y -axis indicates the validation loss. “PINN” refers to the original PINN approach, where stacked auto-differentiation is used during training. “Ours” refers to our new method using Gaussian smoothed models and Stein derivative estimators.

The above three figures show that using the Gaussian smoothed model and approximated derivatives does not hurt the model performance. The models trained with our method is competitive compared to the original PINN approach given the same training epochs. From the bottom three figures, it is clear to see that our method is much more efficient compared to the original PINN approach as it does not require stacked back-propagation, especially in the extremely-high-dimensional settings. For example, in the 5000-dimensional case, our model is nearly $100\times$ faster to achieve a validation loss of $1e - 4$.

This observation clearly demonstrates that our method is able to significantly accelerate the training for high-dimensional PDE problems without sacrificing performance. We believe this is an initial step towards efficiently solving the fundamental problem—high-dimensional Schrodinger equation—using deep learning approaches.

5.3 Ablation studies

Since our approach introduces additional hyper-parameters σ (noise level) and K (sample size) and three statistical estimators of the derivatives, we conduct ablation studies in this section to examine the effects of different design choices.

Regarding the choice of derivative estimators. We leverage variance reduction techniques to improve vanilla Stein’s derivative estimators in Section 4.3. To compare different statistical estimators introduced in the paper, we conduct several numerical experiments and study the approximation errors of each estimator.

We experiment with a Gaussian-smoothed model $u(x) = \mathbb{E}_{\delta \sim \mathcal{N}(0, \sigma^2 \mathbf{I})} f(x + \delta)$, where the base neural network $f(x)$ is a randomly initialized and then fixed 5-layer MLP. The input/output dimension is set to 1000/1 respectively. We set the noise level σ to 0.1, which is used in the previous experiments.

We consider the derivative estimators for the gradient $\nabla_x u$ and the Laplace operator Δu . We randomly sample 10^3 points in $[0, 1]^{1000}$. For each sampled point x , we sample 10^5 Gaussian noises and use back-propagation to calculate $\nabla_x u$ and Δu as an oracle. Empirically, we observe the output of the oracle is very stable, whose variance is less than $1e - 7$.

We compute the L_1 distance between the derivatives returned by the oracle and the derivative estimators used in the paper as the evaluation metric. We compare three estimators: a) the vanilla Stein’s Derivative Estimators, defined in Eqn. (7); b) variance-reduced estimators with the control variate method, defined in Eqn. (8) and (9); c) variance-reduced estimators with both the control variate and the antithetic variable method, defined in Eqn. (10) and (11). For each estimator, we vary the sample size K from 8 to 32768.

The results are shown in the first two subfigures of Figure 4. For the first-order derivative, i.e., $\nabla_x u$, the vanilla Stein’s Derivative Estimator is already accurate, and the variance-reduced ones further improve it slightly. For the second-order derivative, i.e., Δu , the vanilla Stein’s Derivative Estimator performs poorly, whose error is larger than $1e-2$ even with sample size $K = 32768$. The control variate method slightly improves, but the resulting estimator is still inaccurate given reasonable sample size. Combining the control variate method with the antithetic variable method significantly reduces the approximation error: The corresponding estimator is $100\times$ more accurate than the vanilla one. These observations suggest that variance reduction is essential in using Stein’s Identity, especially for estimating high-order derivatives.

Regarding the choice of the noise level σ . As discussed in Section 4.2, the noise level σ controls the expressive power of the Gaussian-smoothed model $u(x)$, which will greatly affect the performance of the learned models. To understand the influence of σ during training, we conduct experiments on 1000-dimensional HJB Equation with σ ranging from 0.01 to 10. Except for the noise level σ , all the other training details and hyper-parameters are the same as those in Section 5.2.

The third subfigure in Figure 4 shows the validation loss curves of using different noise levels. It can be seen that the training goes well when $\sigma \leq 1$, and the value of σ does not affect the model’s performance much. However, when σ becomes too large, e.g., $\sigma = 10$, the validation loss remains high at the end of training. This indicates that the solution of the PDE may not be in the function class that the model could express. Note that σ cannot be arbitrarily small because the calculation of the second-order derivatives involves small values, e.g., σ^4 , which will introduce roundoff error when we use float precision.

Regarding the choice of sample size K . In our method, the sample size K is a hyper-parameter that controls the speed-accuracy trade-off. When K is larger, the approximation of the derivatives is more accurate, while the training would be slower. We run experiments on 1000-dimensional HJB equation with the sample size K ranging from 10^2 to 10^4 .

The fourth subfigure in Figure 4 shows the loss curves of using different sample sizes. We can see that the training is not sensitive to the sample size. Even with only 100 samples, our method still works well. This is because the variance-reduced Stein’s Derivative Estimators can provide sufficiently accurate estimation given a small sample size. It should be noted that the sample size we need can be *less than* the input dimension. This property is advantageous when compared with conventional derivative estimation approaches like numerical differentiation.

6 Conclusion

In this paper, we develop a novel approach that can significantly accelerate the training of Physics-Informed Neural Networks. In particular, we parameterize the PDE solution by the Gaussian smoothed model and show that, as derived from Stein’s Identity, the second-order derivatives can be efficiently calculated without back-propagation. Experimental results show that our proposed method can achieve competitive error compared to standard PINN training but is two orders of magnitude faster. We believe this work is an initial step towards efficiently solving the fundamental problem—high-dimensional Schrodinger equation—using deep learning approaches and will address various other challenges met along the way.

References

- [1] Christopher M Bishop et al. *Neural networks for pattern recognition*. Oxford university press, 1995.
- [2] Ting Chen, Simon Kornblith, Mohammad Norouzi, and Geoffrey Hinton. A simple framework for contrastive learning of visual representations. In *International conference on machine learning*, pages 1597–1607. PMLR, 2020.
- [3] Yuyao Chen, Lu Lu, George Em Karniadakis, and Luca Dal Negro. Physics-informed neural networks for inverse problems in nano-optics and metamaterials. *Optics express*, 28(8):11618–11633, 2020.
- [4] Pao-Hsiung Chiu, Jian Cheng Wong, Chinchun Ooi, My Ha Dao, and Yew-Soon Ong. Can-pinn: A fast physics-informed neural network based on coupled-automatic-numerical differentiation method, 2021.
- [5] Jeremy Cohen, Elan Rosenfeld, and Zico Kolter. Certified adversarial robustness via randomized smoothing. In Kamalika Chaudhuri and Ruslan Salakhutdinov, editors, *Proceedings of the 36th International Conference on Machine Learning*, volume 97 of *Proceedings of Machine Learning Research*, pages 1310–1320, Long Beach, California, USA, 09–15 Jun 2019. PMLR.
- [6] Michael Evans and Timothy Swartz. *Approximating integrals via Monte Carlo and deterministic methods*, volume 20. OUP Oxford, 2000.
- [7] George Fishman. *Monte Carlo: concepts, algorithms, and applications*. Springer Science & Business Media, 2013.
- [8] Abraham D Flaxman, Adam Tauman Kalai, and H Brendan McMahan. Online convex optimization in the bandit setting: gradient descent without a gradient. *arXiv preprint cs/0408007*, 2004.
- [9] JM Hammersley and KW Morton. A new monte carlo technique: antithetic variates. In *Mathematical proceedings of the Cambridge philosophical society*, volume 52, pages 449–475. Cambridge University Press, 1956.
- [10] John Hammersley. *Monte carlo methods*. Springer Science & Business Media, 2013.
- [11] Jiequn Han, Arnulf Jentzen, and E Weinan. Solving high-dimensional partial differential equations using deep learning. *Proceedings of the National Academy of Sciences*, 115(34):8505–8510, 2018.
- [12] Ameya D Jagtap, Kenji Kawaguchi, and George Em Karniadakis. Adaptive activation functions accelerate convergence in deep and physics-informed neural networks. *Journal of Computational Physics*, 404:109136, 2020.
- [13] Yuehaw Khoo, Jianfeng Lu, and Lexing Ying. Solving parametric pde problems with artificial neural networks. *arXiv preprint arXiv:1707.03351*, 2017.
- [14] Diederik P Kingma and Jimmy Ba. Adam: A method for stochastic optimization. In *ICLR (Poster)*, 2015.
- [15] Aditi Krishnapriyan, Amir Gholami, Shandian Zhe, Robert Kirby, and Michael W Mahoney. Characterizing possible failure modes in physics-informed neural networks. *Advances in Neural Information Processing Systems*, 34, 2021.
- [16] Yann LeCun, Yoshua Bengio, and Geoffrey Hinton. Deep learning. *nature*, 521(7553):436–444, 2015.
- [17] Bai Li, Changyou Chen, Wenlin Wang, and Lawrence Carin. Second-order adversarial attack and certifiable robustness. 2018.
- [18] Zongyi Li, Nikola Kovachki, Kamyar Azizzadenesheli, Burigede Liu, Kaushik Bhattacharya, Andrew Stuart, and Anima Anandkumar. Fourier neural operator for parametric partial differential equations. *arXiv preprint arXiv:2010.08895*, 2020.

- [19] Sijia Liu, Pin-Yu Chen, Bhavya Kailkhura, Gaoyuan Zhang, Alfred O Hero III, and Pramod K Varshney. A primer on zeroth-order optimization in signal processing and machine learning: Principals, recent advances, and applications. *IEEE Signal Processing Magazine*, 37(5):43–54, 2020.
- [20] Zichao Long, Yiping Lu, and Bin Dong. Pde-net 2.0: Learning pdes from data with a numeric-symbolic hybrid deep network. *Journal of Computational Physics*, 399:108925, 2019.
- [21] Zichao Long, Yiping Lu, Xianzhong Ma, and Bin Dong. Pde-net: Learning pdes from data. In *International Conference on Machine Learning*, pages 3208–3216. PMLR, 2018.
- [22] Lu Lu, Pengzhan Jin, and George Em Karniadakis. Deeponet: Learning nonlinear operators for identifying differential equations based on the universal approximation theorem of operators. *arXiv preprint arXiv:1910.03193*, 2019.
- [23] Zhiping Mao, Ameya D Jagtap, and George Em Karniadakis. Physics-informed neural networks for high-speed flows. *Computer Methods in Applied Mechanics and Engineering*, 360:112789, 2020.
- [24] Chenlin Meng, Yang Song, Wenzhe Li, and Stefano Ermon. Estimating high order gradients of the data distribution by denoising. *Advances in Neural Information Processing Systems*, 34, 2021.
- [25] George S Misyris, Andreas Venzke, and Spyros Chatzivasileiadis. Physics-informed neural networks for power systems. In *2020 IEEE Power & Energy Society General Meeting (PESGM)*, pages 1–5. IEEE, 2020.
- [26] Yurii Nesterov and Vladimir Spokoiny. Random gradient-free minimization of convex functions. *Foundations of Computational Mathematics*, 17(2):527–566, 2017.
- [27] Tianyu Pang, Kun Xu, Chongxuan Li, Yang Song, Stefano Ermon, and Jun Zhu. Efficient learning of generative models via finite-difference score matching. *Advances in Neural Information Processing Systems*, 33:19175–19188, 2020.
- [28] Adam Paszke, Sam Gross, Francisco Massa, Adam Lerer, James Bradbury, Gregory Chanan, Trevor Killeen, Zeming Lin, Natalia Gimelshein, Luca Antiga, et al. Pytorch: An imperative style, high-performance deep learning library. *Advances in neural information processing systems*, 32:8026–8037, 2019.
- [29] Maziar Raissi, Paris Perdikaris, and George E Karniadakis. Physics-informed neural networks: A deep learning framework for solving forward and inverse problems involving nonlinear partial differential equations. *Journal of Computational Physics*, 378:686–707, 2019.
- [30] Yeonjong Shin, Jerome Darbon, and George Em Karniadakis. On the convergence and generalization of physics informed neural networks. *arXiv e-prints*, pages arXiv–2004, 2020.
- [31] Justin Sirignano and Konstantinos Spiliopoulos. Dgm: A deep learning algorithm for solving partial differential equations. *Journal of computational physics*, 375:1339–1364, 2018.
- [32] Charles M Stein. Estimation of the mean of a multivariate normal distribution. *The annals of Statistics*, pages 1135–1151, 1981.
- [33] Pascal Vincent, Hugo Larochelle, Yoshua Bengio, and Pierre-Antoine Manzagol. Extracting and composing robust features with denoising autoencoders. In *Proceedings of the 25th international conference on Machine learning*, pages 1096–1103, 2008.
- [34] Greg Yang, Tony Duan, J Edward Hu, Hadi Salman, Ilya Razenshteyn, and Jerry Li. Randomized smoothing of all shapes and sizes. In *International Conference on Machine Learning*, pages 10693–10705. PMLR, 2020.
- [35] XIA Yang, Suhaib Zafar, J-X Wang, and Heng Xiao. Predictive large-eddy-simulation wall modeling via physics-informed neural networks. *Physical Review Fluids*, 4(3):034602, 2019.
- [36] Runtian Zhai, Chen Dan, Di He, Huan Zhang, Boqing Gong, Pradeep Ravikumar, Cho-Jui Hsieh, and Liwei Wang. Macer: Attack-free and scalable robust training via maximizing certified radius. *arXiv preprint arXiv:2001.02378*, 2020.